Molecular Crystals and Liquid Crystals Science and Technology. Section A. Molecular Crystals and Liquid Crystals
Publication details, including instructions for authors and subscription information:
http://www.tandfonline.com/loi/gmcl19

Polymorphism and Pseudopolymorphism of the Antibacterial Nitrofurantoin

Mino R Caira [a] , Eduard W Pienaar [b] & Antonie P Lötter [b]
[a] Department of Chemistry, University of Cape Town, Rondebosch, 7700, South Africa
[b] Research Institute for Industrial Pharmacy, Potchefstroom University for CHE, Potchefstroom, 2520, South Africa
Version of record first published: 04 Oct 2006.

To cite this article: Mino R Caira , Eduard W Pienaar & Antonie P Lötter (1996): Polymorphism and Pseudopolymorphism of the Antibacterial Nitrofurantoin, Molecular Crystals and Liquid Crystals Science and Technology. Section A. Molecular Crystals and Liquid Crystals, 279:1, 241-264

To link to this article: http://dx.doi.org/10.1080/10587259608042194

Mol. Cryst. Liq. Cryst., 1996, Vol. 279, pp. 241–264
Reprints available directly from the publisher
Photocopying permitted by license only

POLYMORPHISM AND PSEUDOPOLYMORPHISM OF THE ANTIBACTERIAL NITROFURANTOIN

MINO R CAIRA,[a] EDUARD W PIENAAR[b] and ANTONIE P LÖTTER[b]
[a]Department of Chemistry, University of Cape Town, Rondebosch 7700, South Africa
[b]Research Institute for Industrial Pharmacy, Potchefstroom University for CHE, Potchefstroom 2520, South Africa.

Abstract A physicochemical study of six crystalline modifications of the drug nitrofurantoin is presented. These forms comprise two polymorphs, two monohydrates, a DMF solvate and a DMSO solvate. The clathrate nature of the solvates as well as their thermal decompositions are described. The results of dissolution rate measurements for the polymorphs and monohydrates are discussed in relation to the formulation of the drug.

INTRODUCTION

For drugs having low aqueous solubility, the rate-determining step in bioabsorption is frequently the dissolution rate of the solid drug.[1] This, in turn, depends on the specific polymorph of the drug used in the solid dosage form.[2-4] For a given drug, lack of information on the properties of such forms and their possible interconversions can result in failure to prepare tablets and capsules with reproducible behaviour. A comprehensive study of the polymorphism and pseudopolymorphism of a drug, including the isolation and characterization of its various crystal forms may uncover species with significantly different properties, including dissolution profiles, and is therefore important in the pharmaceutical industry.[5] Pseudopolymorphic (solvated) forms of drugs are frequently encountered during crystallization of the drug from different solvents. Pseudopolymorphs such as hydrates also find use in drug preparations. Such species are supramolecular systems and are of interest as such, or as models for drug-receptor interactions.[6]

In this paper, we report on the polymorphism and pseudopolymorphism of nitrofurantoin, [N-(5-nitro-2-furfurylidene)-1-aminohydantoin], Fig.1, a widely used nitrofuran antibiotic which is active against many urinary tract pathogens.[7] Hitherto, nitrofurantoin was known to exist in a monohydrous and an anhydrous form, and previous studies by a number of authors[8-12] reported their physical data as well as bioavailability problems associated with the drug.

Pseudopolymorphs of nitrofurantoin containing N,N-dimethylformamide (DMF) and dimethylacetamide (DMA) were also reported[13] but were not regarded as being of pharmaceutical interest owing to the toxicity of the included solvents.

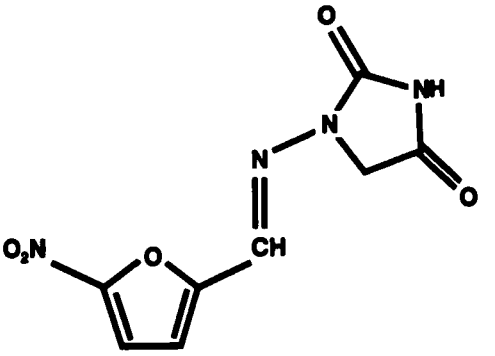

FIGURE 1 Structural formula of nitrofurantoin.

We recently reported the conditions for isolating four modifications of nitrofurantoin, namely two anhydrous forms[14] designated α and β, and two monohydrates,[15] I and II, as well as the single crystal X-ray structures of these species. Here, we present their physicochemical characterization by scanning electron microscopy (SEM), hot stage microscopy (HSM), thermogravimetric analysis (TGA), differential scanning calorimetry (DSC), X-ray powder diffraction (XRD) and IR-spectroscopy, and we attempt to relate these data to the known crystal structures. In addition, we report the single crystal X-ray structures of two pseudopolymorphs, III and IV, obtained by recrystallizing the drug from dimethylformamide (DMF) and dimethylsulphoxide (DMSO) respectively, and the investigation of their thermal decomposition by HSM, DSC and XRD methods. A scheme summarising the relationships between the various nitrofurantoin species isolated is presented. Finally, the dissolution rate data for the forms α, β, I, and II are presented and their practical implications for the formulation of nitrofurantoin are discussed.

EXPERIMENTAL

Crystal preparation and physical characterization

The raw material (Sigma Chemical Co., USA, Lot no.67F-0765) was identified by TG, DSC and XRD methods as the β-polymorph of nitrofurantoin. Preparation of single crystals of the forms α, β, I, and II were described earlier.[14,15] For III, 300 mg

nitrofurantoin were dissolved in 7.5 cm^3 dry DMF with stirring at 60°C for 5 min. Single crystals grew from the solution maintained at 40°C. Single crystals of IV were obtained by slow evaporation of a solution made by dissolving 200 mg nitrofurantoin in 2.5 cm^3 dry DMSO at room temperature (20°C).

SEM photomicrographs were taken using a Stereoscan 250 instrument (Cambridge Scientific Instruments, Cambridge, UK).

HSM observations were made at variable heating rates (1 - 10°C min^{-1}) using a Leitz (Laborlux K) hot stage microscope. Thermal analysis was performed on a Perkin Elmer PC Series 7 system. For TGA, samples (2-3 mg) were heated in Pt pans at 10°C min^{-1}. For DSC, 2-3 mg samples were sealed in Al pans and heated at 10°C min^{-1} using an empty pan as reference. Nitrogen purge gas flowing at 20 cm^3 min^{-1} was used for both TGA and DSC.

XRD patterns were recorded on a Philips PW1050/80 goniometer using Ni-filtered CuKα-radiation (λ = 1.5418Å). Calculated XRD patterns were obtained with program Lazy Pulverix.[16] Input data included unit cell parameters, space group, atomic positions and thermal parameters obtained from the single crystal X-ray analyses.[14,15]

IR-spectra were recorded on a Perkin Elmer 983 double beam spectrometer using Nujol mull samples placed between NaCl plates.

For the solubility study, the same fraction (100-150μm) was used for all modifications. An amount of drug which ensured supersaturation was mixed with 10 cm^3 H_2O and sealed in ampoules rotated at 30 r.p.m. in a thermostated bath at 25°C for 7 days. The solution concentrations were determined spectrophotometrically by absorbance measurements at 375 nm using a Shimadzu (UV-160) spectrophotometer. Intrinsic dissolution rates (IDR) were determined by the methods of Simonelli et al.[17] and Singh et al.[18] The sample powder was compressed into a tablet in a 13 mm die at 7 MPa. The back of the die was sealed and mounted directly in a water-jacketed beaker containing 300 cm^3 of distilled H_2O thermostatically controlled at 37$\pm$1°C. A stirrer operating at 150 r.p.m. and placed 6 mm from the tablet surface was used. Samples were withdrawn at various time intervals and the assay performed spectrophotometrically. Prior to the study, samples of all modifications were compressed at 7 MPa to assess whether pressure might result in polymorphic changes. Comparison of XRD spectra of the compressed samples with those calculated from the crystal structures confirmed that there were no changes.

For powder dissolution rate measurements, the same particle size fraction (100-150 μm) was used for all modifications. The method described by Lötter et al.[19] was used for dissolution rate measurements with apparatus no.2 of the USP.[20] Five mg of

each sample was introduced into 1 dm^3 of distilled H_2O at 37±1°C and a stirring speed of 100 r.p.m. was used. Aliquots of 5 cm^3 were withdrawn at various time intervals, filtered and assayed with the same procedure described for the IDR determination. Each determination was carried out six times and was corrected for dilution.

Single crystal X-ray analyses of III and IV

These followed analogous standard direct methods[21] and least-squares refinement[22] procedures using data collected at 294K on an Enraf-Nonius CAD4 diffractometer with MoKα-radiation (λ= 0.7107Å). For both crystals, data were collected in the range $1° \leq \theta \leq 25°$ using the ω-2θ scan mode with variable scan width, aperture width, and speed. All data were corrected for Lorentz-polarization effects. The data for III were corrected for intensity decay (10.1%) and those for IV for absorption.

The analysis of IV revealed the O atom of DMSO on a diad, the S atom disordered over two sites, and the C atom in a general position. H atoms in III and IV were located in difference electron density maps but were included in idealized positions with C-H, N-H 1.00Å in a riding model. The criterion for observed reflections was $I > 2\sigma(I)$.

All non-H atoms were treated anisotropically and H atoms were assigned common variable U_{iso} values for chemically different groups. Weights of the form $w = [\sigma^2(F_o) + gF_o^2]^{-1}$ were employed. Structure factor tables, thermal parameters, atomic coordinates and derived molecular parameters for III and IV are available from the authors.

RESULTS AND DISCUSSION

Physicochemical characterization of crystal forms α, β, I, II

The use of several physical methods to distinguish the various forms of nitrofurantoin are discussed below; where possible, the analytical results are interpreted on the basis of the known crystal structures of these forms.[14,15]

Crystal habits of nitrofurantoin are known to be affected by recrystallization conditions.[13] SEM photographs of the crystals obtained by the procedures we described earlier[14,15] are shown in Fig.2. The distinctive habits (plates, tabular crystals, rhombs and needles respectively) aid in the identification of these phases.

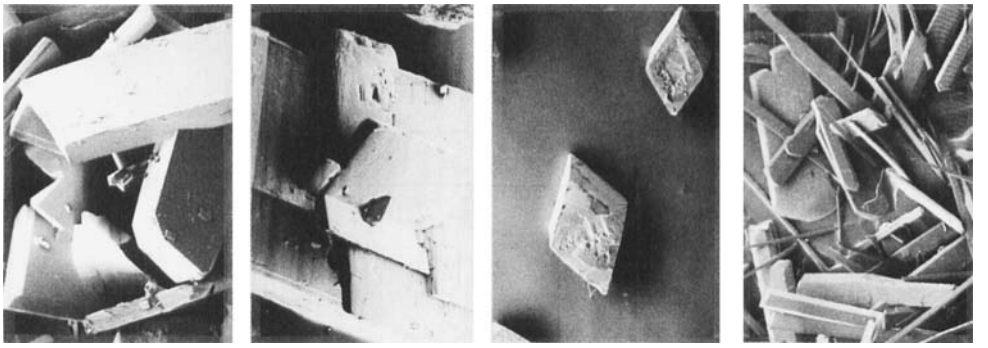

FIGURE 2 SEM photographs of nitrofurantoin crystal modifications (20 x). Left to right: α, β, I, II.

On the hot stage, crystals of the α-polymorph turned brown and melted at 268°C and the sample transformed into a dark brown liquid at 270°C. Identical changes were recorded for the β-polymorph at 270 and 271°C respectively. On heating crystals of the monohydrate I, they became opaque at 108°C and turned brown and melted in the range 272-273°C. At 274°C, the entire sample transformed into a dark brown liquid. Crystals of II underwent identical changes at temperatures 128, 271 and 273°C respectively. The changes occurring at 108°C for I and at 128°C for II were assumed to be dehydration since bubbles of vapour appeared when the crystals were heated under silicone oil. The colour changes accompanying melting were taken as evidence of simultaneous decomposition of the drug. Heating any of the four forms in the temperature range 250-320°C resulted in significant weight loss after fusion, confirming subsequent drug decomposition. These transformations were studied quantitatively by TGA and DSC methods.

The TGA traces for polymorphs α and β showed zero weight loss in the range 25-250°C, confirming that these phases are free of included solvent. Their DSC traces are shown in Fig.3. These have similar features, namely a sharp endotherm corresponding to fusion followed by a large, sharp exotherm associated with decomposition. No transition point representing a transformation from one polymorph to the other was detected in either DSC trace. Similar behaviour has been observed for polymorphs of other drugs.[23,24] The peak melting temperatures are very close (α 275, β 270°C) and the crystal densities of 1.656 and 1.648 g cm^{-3} differ by only 0.5%. These data suggest that the α form has only a slightly greater stability than the β form and that the packing energies of the two crystals are very similar. Inspection of the crystal packing diagrams, Fig.4, shows that both polymorphs consist of closely

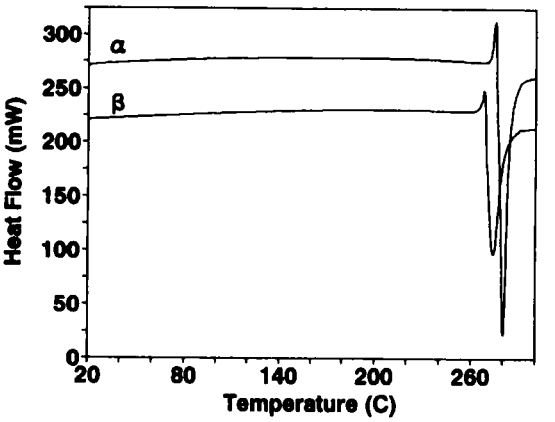

FIGURE 3 DSC traces for polymorphs α and β.

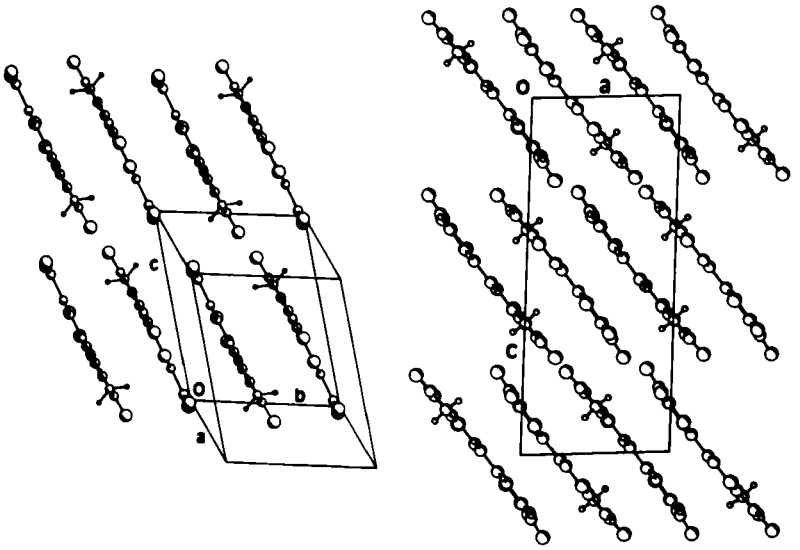

FIGURE 4 Layer structures of (left) α-, (right) β-polymorphs of the drug. (Reproduced from Ref. 15, with permission).

stacked layers of planar nitrofurantoin molecules. The hydrogen bonding arrangements within the respective layers are different, but the number and types of intermolecular hydrogen bonds (N-H···O, C-H···O) in which each drug molecule engages is the same in the two forms. The crystal structure of the β-polymorph was determined independently by Bertolasi et al.,[25] but they did not state how this polymorph was prepared. However, the presence of centrosymmetrically stacked layers in the crystal was rationalised on the basis of INDO calculations which yielded a very large value of 8.11D for the dipole moment between two inversion-related molecules. It is likely that this favourable interaction is one of the factors determining the type of stacking we have observed in nitrofurantoin crystal modifications.[14,15]

TGA traces for the monohydrates are shown in Fig.5. In both cases there is an overall measured weight loss of 7.0%, which is consistent with a calculated value of 7.03% for the loss of 1 mol water per mol of drug. However, monohydrate I is seen to lose water more rapidly than II. This is reflected in the DSC traces, Fig.6, which

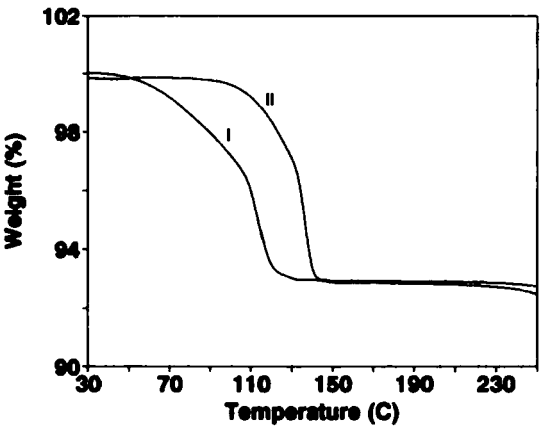

FIGURE 5 TGA traces for nitrofurantoin monohydrates I and II.

show dehydration endotherms at significantly different temperatures of 104°C for I and 127°C for II, with measured ΔH values of 26.1 and 36.4 kJ mol^{-1}. After dehydration, the samples melted at 271 and 273°C respectively, these temperatures lying between the melting points of polymorphs α and β. It was therefore not possible to identify the polymorphic forms of the dehydrated species unequivocally from the DSC data and XRD (below) was employed for this purpose.

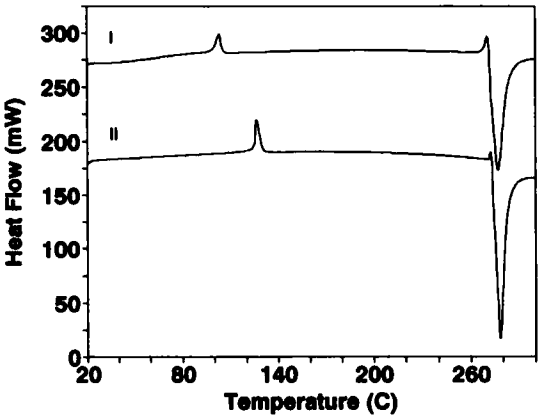

FIGURE 6 DSC traces for nitrofurantoin monohydrates I and II.

To rationalise the lower temperature and enthalpy of dehydration for monohydrate I, we compared the crystal structures of I and II. These monohydrates have distinctly different packing arrangements,[14] I possessing a layer structure similar to those of the polymorphs, while in II a herringbone motif occurs. The included water molecules play a major role in stabilizing the crystal structures. Detailed studies by Perrier and Byrn[26] on the thermal decomposition of drug hydrates showed that dehydration onset temperatures can be correlated with the cross sectional area of water tunnels in hydrate crystals and the number and strengths of hydrogen bonds to water molecules. Our comparison of the hydrogen bond data[14] for the monohydrate crystals I and II shows that when the overall number and strengths (as measured by N···O, C···O distances) of these interactions are considered, the crystal cohesion they provide is not very different for the two forms. A reasonable explanation for the different dehydration behaviours was found by inspecting the modes of water inclusion. Using program MOLMAP,[27] sections through both crystals were drawn with the atoms represented as spheres with van der Waals radii, to reveal the presence of channels or cavities. Whereas water molecules are contained in isolated cavities in II, in species I they are located in continuous channels, as shown in Fig.7. It is likely that the existence of such channels in I (and their absence in II) is the principal factor facilitating the escape of water on heating the crystals of I, resulting in a lower temperature and ΔH of dehydration compared with those for II.

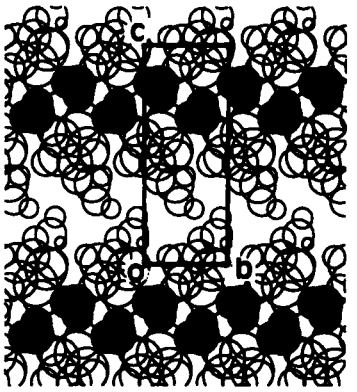

FIGURE 7 Water molecules (shaded) located in channels in monohydrate I.

IR-spectra for the polymorphs and monohydrates are shown in Figs. 8 and 9 respectively. Table I lists several bands which may be used to distinguish the polymorphs. The splitting of the C=O band in the β-form is consistent with the two significantly different C=O distances (1.192(4), 1.216(3)Å) found in the crystal.[15] The polymorphs are readily distinguished from the monohydrates since the latter show characteristic bands in the O-H stretching region. Furthermore, these bands occur at 3535 and 3440 cm^{-1} in I but are shifted to 3620 and 3470 cm^{-1} in II, allowing the

TABLE I Wavenumbers (cm^{-1}) for assigned IR-bands

Assignment	α	β
N-H stretch	3160	3260
C=O stretch	1660	1660
		1673
C-N stretch	1130	1108
N-H bend	743	720

monohydrates to be distinguished from each other. The major peak shifts or splittings indicated in Figs. 8 and 9 facilitate the identification of the four individual forms.

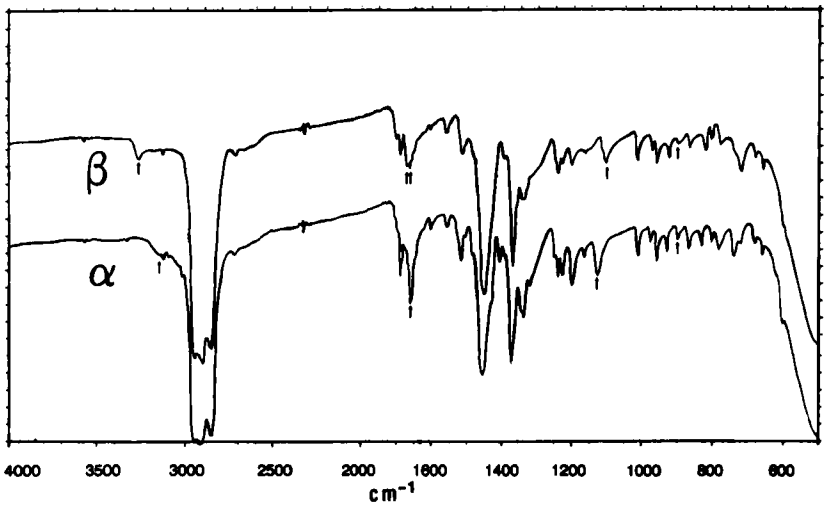

FIGURE 8 IR-spectra for the α- and β-polymorphs.

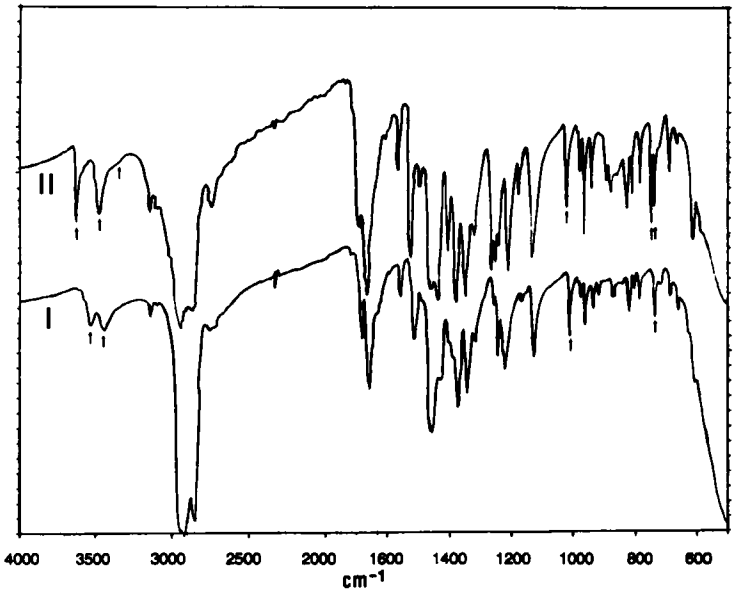

FIGURE 9 IR-spectra for the monohydrates I and II.

The XRD method was found to be the most reliable method for identifying these species. In Fig.10, the calculated XRD patterns based on the single crystal X-ray data for the four phases are given as the best representations of the pure phases.[28] While the main practical use of the XRD patterns is in future phase identification, we note that the most prominent features of the patterns can be explained in terms of the known crystal structures. For example, the strongest peak in the patterns for the α- and β-polymorphs occurs at almost identical 2θ-values corresponding to d-spacings of 3.112 and 3.098Å respectively. As expected, the respective sets of planes in these phases, namely (0 2 1) and (2 0 -4), are those containing the closely packed layers of nitrofurantoin molecules. In Fig.4, the view direction is parallel to these planes. The most intense peak in the pattern for Form I has d = 3.114Å and the planes (3 0 1) in this phase contain similar molecular layers. For II, the second most intense peak contains the (0 2 4) and (0 -2 4) reflections with d = 3.259Å. These are again associated with closely spaced layers of drug molecules parallel to the two directions defined by the herringbone arrangement. Thus, the layer stacking in all of these phases is prominently featured in their XRD patterns.

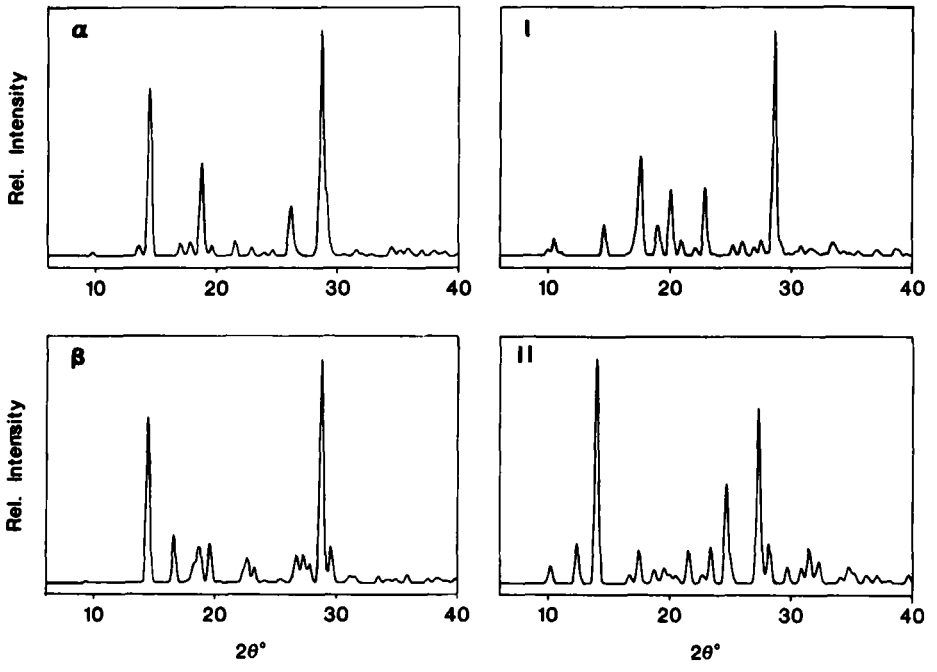

FIGURE 10 XRD patterns for α, β, I and II, calculated from their single crystal X-ray structures.

Controlled dehydration of monohydrates I and II by heating at 120°C(I) and 110°C(II) in vacuum (1 mmHg) for 30 min yielded powders whose XRD patterns matched that of the β-polymorph of the drug.

Physicochemical characterization and X-ray crystal structures of pseudopolymorphs III and IV

The XRD traces for III and IV, obtained by recrystallization from DMF and DMSO respectively, are shown in Fig.11. These differ significantly from those of the forms α, β, I, and II, indicating that III and IV are new phases. Prominent peaks at 2θ = 28.4° (d=3.14Å) for III and 28.1° (d=3.18Å) for IV suggested, by analogy with the patterns for α, β, I, and II, that these crystals might contain closely packed layers of drug molecules.

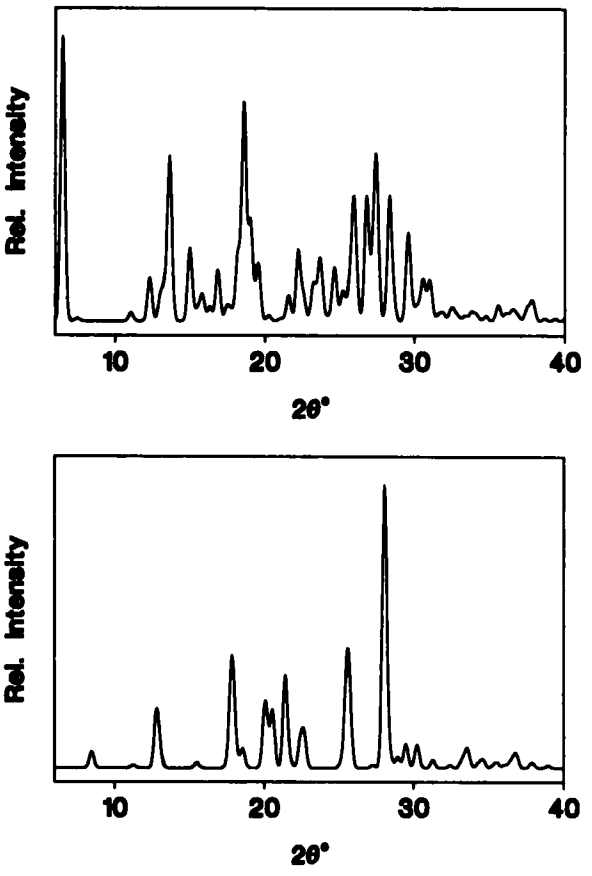

FIGURE 11 XRD patterns for pseudopolymorphs III (upper) and IV (lower).

On heating crystals of III on the hot stage, they became opaque at 123°C. At 259°C they changed colour from orange to brown and melting commenced at 277°C. Species IV became opaque at 188°C and commenced melting at 273°C. Fig. 12 shows combined TGA-DSC traces for these species. The measured weight loss for III was 23.0%, in excellent agreement with a calculated value of 23.5% for a 1:1 nitrofurantoin DMF solvate. For IV, the experimental weight loss was 14.6% versus a calculated value of 14.1% for a 2:1 nitrofurantoin DMSO complex. From TGA, III

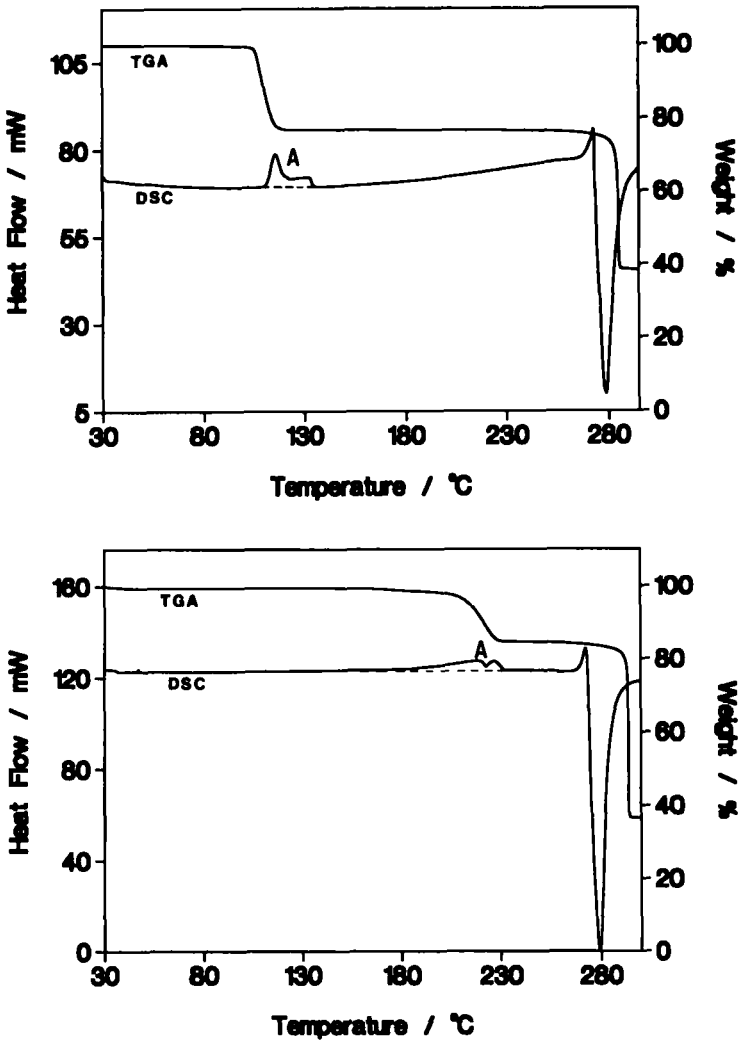

FIGURE 12 Combined TGA-DSC traces for the pseudopolymorphs III (upper) and IV (lower).

desolvated over the low temperature range of 100-125°C whereas for IV the range was 160-235°C. This striking difference was reflected in the DSC traces where the desolvation endotherm temperature ranges were 109-137°C (III) and 180-234°C(IV). In both cases, these endotherms (labelled A) consist of two peaks, indicating complex desolvation mechanisms. We have used the parameter T_{on} - T_b (T_{on} = onset temperature for desolvation, T_b = boiling point of pure solvent) as a measure of the thermal stability of an inclusion compound.[29] The value of this parameter is about -41°C for III and +14°C for IV, indicating a much greater stability for IV, the complex containing DMSO. The fusion endotherm for both species occurred at 273°C and the decomposition exotherms peaked at 279°C. Controlled desolvation by heating III at 195°C and IV at 240°C for 1h removed all traces of solvent and the XRD patterns of the desolvated powders matched that of the β-polymorph of nitrofurantoin.

Table II lists crystal data and details of data-collection parameters and refinements for III and IV. The asymmetric unit of III, shown in Fig. 13 consists of two nitrofurantoin molecules and two DMF molecules. Bond lengths and bond angles for the independent host drug molecules are not significantly different and agree with those observed in the other forms of nitrofurantoin.[14,15] Both of the DMF molecules are planar, the maximum deviation of a non-hydrogen atom from either of the mean planes being 0.03Å. The drug molecules maintain the same, essentially planar

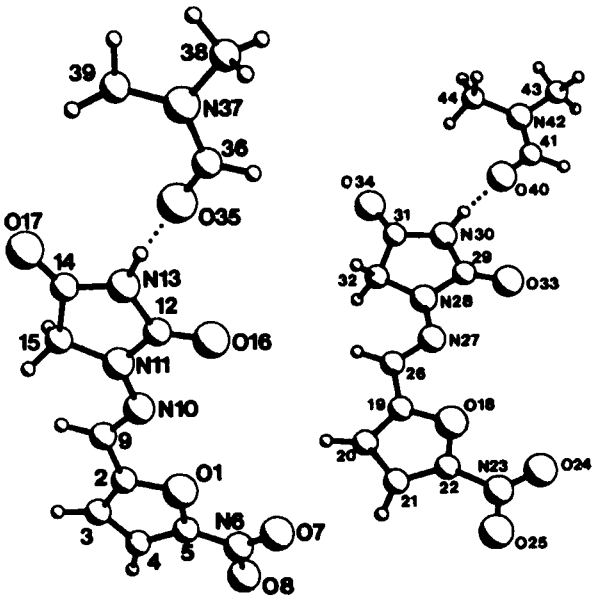

FIGURE 13 The asymmetric unit in crystals of III.

TABLE II Crystal data, details of data-collection and refinement for pseudopolymorphs III and IV.

	III	IV
Formula	$C_8H_6N_4O_5 \cdot (C_3H_7NO)$	$C_8H_6N_4O_5 \cdot (C_2H_6SO)_{0.5}$
M_r/g mol^{-1}	311.25	277.22
a/Å	8.038(2)	16.401(5)
b/Å	13.006(9)	13.838(3)
c/Å	15.027(5)	10.344(4)
α/°	114.45(5)	90.0
β/°	94.22(3)	102.50(3)
γ/°	90.89(4)	90.0
V/Å^3	1424(1)	2292(1)
Z	4	8
Space group	$P\bar{1}$	C2/c
μ(MoKα)/cm^{-1}	1.12	2.09
F(000)	648	1144
D_x/g cm^{-3}	1.451	1.607
Crystal size/mm	.38 x .28 x .28	.22 x .34 x .16
Reflections measured	5233	2235
Unique reflections	4091	1860
R_{int}	0.019	0.027
Observed reflections	2861	1626
Parameters refined	417	181
Max Δ/σ	0.60	0.01
R	0.064	0.045
R_w	0.067	0.055
S	3.138	0.614
$\Delta\rho$/eÅ^{-3},min,max	-.15, .14	-.34, .24

conformation observed in Forms α, β, I, and II (that shown in Fig.1) with all torsion angles deviating by less than 10° from 0 or 180°. The nitro-substituents are twisted slightly out of the furan plane in opposite directions in the two independent molecules. The principal host-guest interaction is a host(N-H)···O(guest) hydrogen bond which occurs in both independent complex units as indicated in Fig.13. Hydrogen bond data are listed in Table III. The triclinic unit cell of III (Table II) is pseudo-monoclinic.

TABLE III Hydrogen bond data for III and IV (distances Å, angles °)

III

D-H···A	D-H	D···A	H···A	D-H···A
N(13)-H(13)···O(35)^{i}	1.00	2.688(7)	1.691(7)	173.9(4)
C(3)-H(3)···O(34)^{ii}	1.00	3.180(7)	2.188(6)	171.0(5)
N(30)-H(30)···O(40)^{iii}	1.00	2.695(8)	1.697(8)	174.1(5)
C(20)-H(20)···O(17)^{iv}	1.00	3.187(7)	2.201(6)	168.7(6)

(i): -1+x, y, 1+z (ii): 1-x, 2-y, 2-z
(iii): 1+x, y, 1+z (iv): -x, 2-y, 2-z

IV

D-H···A	D-H	D···A	H···A	D-H···A
N(13)-H(13)···O(20)^{i,ii}	1.00	2.788(3)	1.808(3)	165.6(2)
C(9)-H(9)···O(8)^{iii}	1.00	3.293(2)	2.529(2)	133.0(2)
C(9)-H(9)···O(17)^{iv}	1.00	3.249(2)	2.467(2)	134.7(2)

(i): -x, 1-y, -z (ii): x, 1-y, -1/2+z
(iii): x, -y, -1/2+z (iv): x, -y, 1/2+z

A prominent feature observed in X-ray precession photographs was the systematically low intensities of reflections 0kl with k = 2n+1, indicating a pseudo b-glide plane normal to the a-axis. This pseudosymmetry relates the complex units shown in Fig.13. The crystal packing arrangement, Fig.14, shows the drug molecules drawn in stick-representation while the guest DMF molecules are drawn in space-filled representation. This emphasises the clathrate nature of III with guest molecules trapped in channels parallel to the a-axis formed by barriers of planar host drug molecules. The latter form closely stacked layers in two orientations similar to the arrangement observed in monohydrate II. Each host drug molecule is linked to another host molecule by a

C-H···O hydrogen bond only, involving equivalent atoms H(3) and H(20) of the two independent molecules.

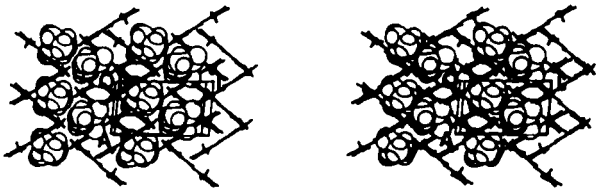

FIGURE 14 Stereoview of the crystal packing in III.

Fig.15 shows the 2:1 drug:solvent complex in IV. The O atom of the DMSO molecule is located on a diad. This atom is the donor in two equivalent hydrogen bonds N(13)-H(13)···O(20) to diad-related drug molecules. The DMSO molecule is

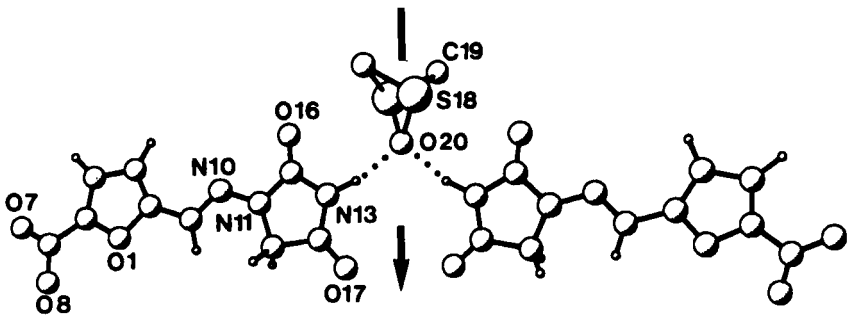

FIGURE 15 The 2:1 nitrofurantoin-DMSO complex unit in IV showing the C_2 symmetry of the disordered DMSO.

disordered, the S atom occupying two alternative positions about the diad. The molecular geometry is normal, however, with distances S=O 1.563(3)Å, S-C 1.745(3)Å. The drug molecules are again in a planar conformation but one which is unique in the series of nitrofurantoin modifications we have studied. Here, the O(1)-C(2)-C(9)-N(10) grouping is anti-planar (Fig.15) whereas it is syn-planar (Fig.1) in the polymorphs, the monohydrates and complex III. The crystal packing diagram is shown in Fig.16 from which the clathrate nature of IV is evident. DMSO molecules of alternating orientation along the y-direction occupy channels parallel to the c-axis of the crystal. In contrast to III, the drug molecules in IV stack in layers with a common

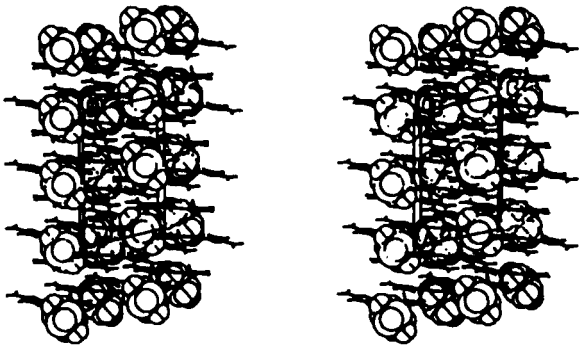

FIGURE 16 Stereoview of the crystal packing in IV.

orientation. The only host-host interaction is a bifurcated C-H···O hydrogen bond involving the acidic atom H(9) (Table III). We noted previously[14,15] for crystals of species α, β, I, and II, that in addition to host intermolecular N-H···O hydrogen bonding, C-H···O hydrogen bonding (involving H(9) specifically) invariably occurs and concluded that it plays an important role in stabilizing the crystal structures. The only species in which atom H(9) does not participate in hydrogen bonding is III, which is nevertheless stabilized by both N-H···O and C-H···O hydrogen bonds. Pseudopolymorphs III and IV may be described as coordinato-clathrates in a coordination-assisted host lattice,[30] where the first interaction, host(N-H)···O(guest), is stronger than the second, host(C-H)···O(host).

Channel topologies in III and IV were investigated in order to explain the considerable difference in the thermal stabilities of these clathrates. The relevant sections through these crystals are shown in Fig.17. Detailed analysis of the topologies of the channels revealed that they are constricted, with a slightly looser fit of the DMF molecules compared with DMSO so that, assuming escape of the guest molecules along these channels on heating, the DMF molecules might more readily be lost. However, the relatively small differences in channel topology alone are unlikely to account for the large difference in the measured T_{on} - T_b values and a more likely explanation for the relative ease of loss of DMF compared with DMSO is the fact that each DMF molecule in III is bound to a host molecule by only one N-H···O hydrogen bond whereas each DMSO molecule in IV engages in two N-H···O hydrogen bonds to host molecules. The greater stability of the DMSO solvate was also reflected in a simple competition experiment in which nitrofurantoin was dissolved in an equimolar mixture of DMF and

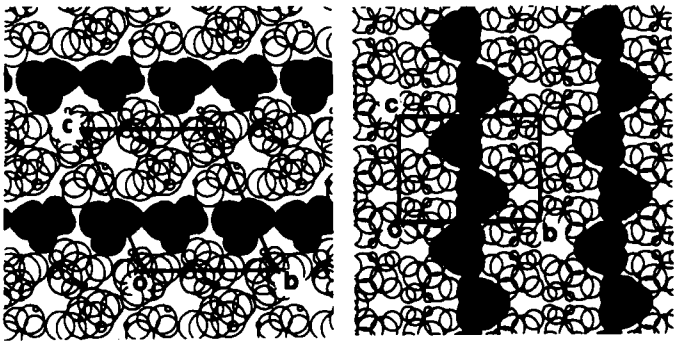

FIGURE 17 Channel occupation by solvent molecules (shaded) in crystals of III (left) and IV (right).

DMSO. It was confirmed by TGA, DSC and XRD that the species which crystallized preferentially and exclusively was the DMSO solvate IV.

Attempts to observe a solvent front by HSM as evidence for solvent escape along specific morphological directions in the crystals were unsuccessful. We have, however, demonstrated that loss of DMF and DMSO on heating III and IV respectively results in collapse of their crystal structures to the β-polymorph of the drug and that for IV, the rearrangement is accompanied by a change in the conformation of the nitrofurantoin molecule.

Dissolution rates and phase transformations of nitrofurantoin crystal modifications

A study of the solubility and dissolution rates of forms α, β, I, and II of the drug was carried out since previous studies[10,31] which referred to only one polymorph and one monohydrate form, are necessarily incomplete in this respect. Furthermore, having established the conditions for obtaining the four distinct forms of the drug, we regarded the determination of their dissolution rates as an important objective in view of the current usage of the drug. Some patients have experienced nausea and emesis on nitrofurantoin administration and there is evidence that this undesirable effect may be of neural origin. The rate of absorption has been indicated as a probable factor.[32] One approach to this problem is the use of larger crystals (80-200 mesh) having less surface area per dose and showing a consequent reduction in absorption rate. This has been shown to reduce the incidence of emesis, with ample urinary excretion rate.[32]

Reduction of side-effects thus requires control of the crystal size with marketed products which normally contain the β-polymorph.

Aqueous solubilities at 25°C for the four drug modifications did not vary significantly, ranging from 75(2)-82(2) μg cm^{-3}. A possible explanation for the results of this equilibrium study is that the anhydrous forms transformed into a hydrate and that, at the end of the seven-day experiment, the solubilities of only the hydrated forms were in fact determined. The intrinsic dissolution rates (IDR) measured at 37±1°C using prepared tablets were: α 34.7(7), β 48.2(8), I 36.6(7), and II 39.3(4) μgcm^{-2}min^{-1}. A statistical evaluation of the IDR data was performed using Tukey's studentized range test; no significant differences ($p < 0.05$) were found when comparing forms α, I, and II. However, the IDR for the β-polymorph was significantly higher than those of the other forms. The mean IDR curves are shown in Fig.18. A statistical analysis of the powder dissolution rate data yielded analogous

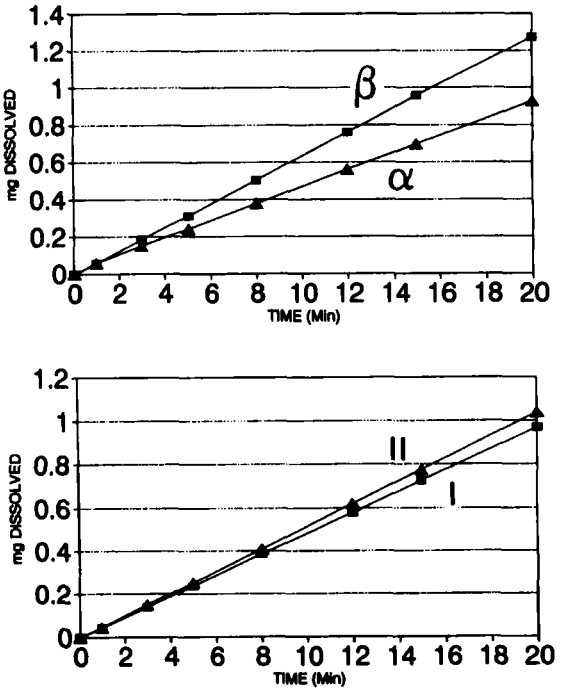

FIGURE 18 Mean intrinsic dissolution rate curves for forms α, β, I, and II of nitrofurantoin.

results. Fig. 19 shows the mean powder dissolution rate curves for the four modifications. The results are consistent with data for the two forms of the drug

studied previously: Otsuka et al.[10] found that the dissolution rate of a monohydrate (identified as Form II in our study) was significantly less than that of an anhydrous form (identified as β in our study). According to these authors, the dissolution of the anhydrous form involves crystallization with a transformation to a hydrated form. We have confirmed by DSC analysis of the surfaces of tablets used for IDR measurements that both the α- and β-polymorphs transform to monohydrate II .

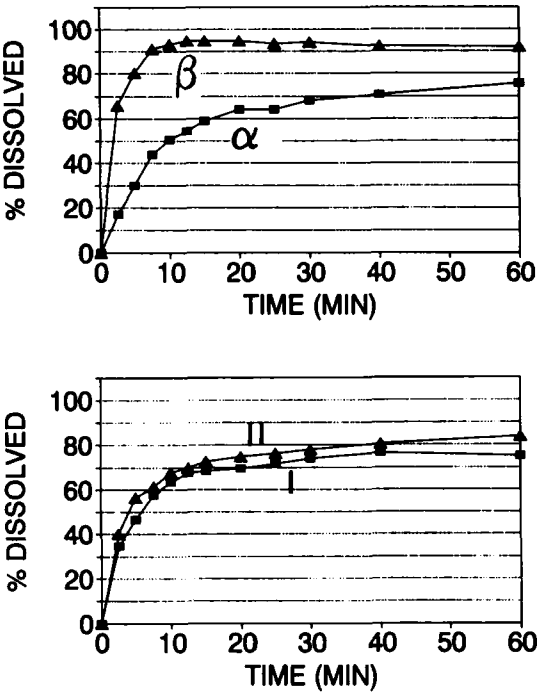

FIGURE 19 Mean powder dissolution rate curves for forms α, β, I and II of nitrofurantoin.

The more rapid initial dissolution rate of the β-polymorph (the form normally used in marketed dosage forms) may be related to the incidence of adverse side-effects described earlier.[32] Our results, which demonstrate the retarded dissolution rates of Forms α, I, and II relative to the β-polymorph therefore indicate that these three forms may be more favourable for pharmaceutical formulation and would have the further advantage of not requiring careful control of crystal size in formulation. A bioavailability study is necessary to assess this prediction.

The finding that the dissolution rate of the α-polymorph is significantly less than that of the β-polymorph is unexpected in view of the crystal structure analyses which showed these phases to be comparable in terms of molecular interactions in the solid state. It was, however, demonstrated that both polymorphs transform into monohydrate II under dissolution conditions so that a likely explanation for the apparently different dissolution rates of the polymorphs is that the rates of this transformation differ for α and β. The implication is that α transforms into II more rapidly than β, so that for dissolution of the α-form, what is effectively being measured is the dissolution rate of a rapidly growing layer of II. This would yield comparable dissolution rate curves for forms α and II, as observed, while the dissolution of the β-form would proceed relatively unimpeded in accordance with the general observation that anhydrous forms tend to have higher dissolution rates than hydrated forms.[33] Comparable dissolution rates found for monohydrates I and II, with very similar cohesive interactions in the solid state, are consistent with the remarks above. Separate experiments to measure the kinetics of hydration of the polymorphs are in progress.

A summary of the observed solid state and solvent-mediated phase transformations of nitrofurantoin, including all six crystal modifications characterized in this study, is given in Fig.20. The raw material from which all crystal forms were prepared was the β-polymorph. We note that controlled drying of any solvated form leads to formation of the β-polymorph exclusively, while we have thus far been able to isolate the more stable α-polymorph only by recrystallization from an appropriate medium.[15]

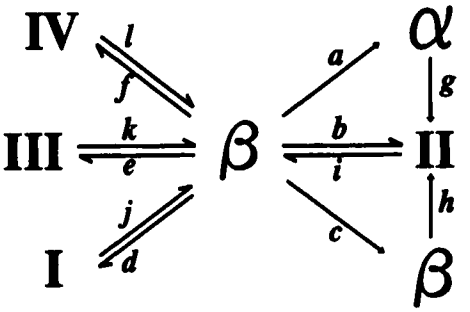

FIGURE 20 Transformations of nitrofurantoin modifications.
a-f: single crystal formation from powdered raw material (β-polymorph);
g,h: hydration of polymorphs;
i-l: desolvation of pseudopolymorphs.

Acknowledgements

We thank the Universities of Cape Town, the University of Potchefstroom for CHE, and the FRD (Pretoria) for financial assistance.

REFERENCES

1. A. Martin, Physical Pharmacy, (Lea & Febiger, Philadelphia,4th Ed. 1993), p.331.
2. J.K. Haleblian, J. Pharm. Sci., 64, 1269(1975).
3. S.R. Byrn. Solid-state chemistry of drugs. (Academic Press, New York, 1982), p.143.
4. L. Borka and J.K. Haleblian, Acta Pharm. Jugoslav., 40, 71(1990).
5. W.I. Higuchi, P.D. Bernardo and S.C. Mehta, J. Pharm. Sci., 56, 200(1967).
6. P.M. Dean, in Molecular Foundations of Drug-Receptor Interaction, (Cambridge University Press, England, 1987), pp188-235.
7. MARTINDALE: The Extra Pharmacopoeia, (The Pharmaceutical Press, London, 28th Ed. 1982), p.1048.
8. M. Otsuka, R. Teraoka and Y. Matsuda, Chem. Pharm. Bull., 38, 833(1990).
9. M. Otsuka, R. Teraoka and Y. Matsuda, Pharm. Res, 8, 1066(1991).
10. M. Otsuka, R. Teraoka and Y. Matsuda, Chem. Pharm. Bull., 39, 2667(1991).
11. M. Otsuka and Y. Matsuda, J. Pharm. Pharmacol, 45, 406(1993).
12. P.V. Marshall and P. York. Int. J. Pharm., 55, 257(1989).
13. N. Garti and F. Tibika, Drug Dev. Indust. Pharm., 6, 379(1980).
14. E.W. Pienaar, M.R. Caira and A.P. Lötter, J. Crystallogr. Spectr. Res., 23, 739(1993).
15. E.W. Pienaar, M.R. Caira and A.P. Lötter, J. Crystallogr. Spectr. Res., 23, 785(1993).
16. K. Yvon, W. Jeitschko and E.J. Parthè, J. Appl. Cryst., 10, 73(1977).
17. A.P. Simonelli, S.C. Mehta and W.I. Higuchi, J. Pharm. Sci., 58, 538(1969).
18. P. Singh, S.J. Desai, D.R. Flanagan, A.P. Simonelli and W.I. Higuchi, J. Pharm. Sci., 57, 959(1968).
19. A.P Lötter, D.R. Flanagan, N.R. Palepu and J.K. Guillory, Pharm. Technol., 7, 56(1983).
20. United States Pharmacopoeia XXII, (Mack Publishing company, Easton, 1990), p.1578.
21. G.M. Sheldrick, SHELX86, (G.M. Sheldrick, C. Kruger and R. Goddard, Eds.) Crystallographic computing 3, (Oxford University Press, 1986), p.175.
22. G.M. Sheldrick, SHELX76, A system of computer programs for X-ray structure determination. (University of Cambridge, England, 1976).
23. J.J. Gerber, M.R. Caira and A.P. Lötter, J. Crystallogr. Spectr. Res., 23, 863(1993).
24. A. Miyamae, S. Kitamura, T. Tada, S. Koda and T. Yasuda, J. Pharm. Sci., 80, 995(1991).
25. V. Bertolasi, P. Gilli, V. Ferretti and G. Gilli, Acta Crystallogr., 49, 741(1993).
26. P.R. Perrier and S.R. Byrn, J. Org. Chem., 47, 4671(1982).
27. Program MOLMAP: L.J. Barbour, (Ph.D Thesis, University of Cape Town, 1994).
28. I. Bar and J. Bernstein, J. Pharm. Sci., 74, 255(1985).
29. M.R. Caira, L.R. Nassimbeni, M.L. Niven, W.-D. Schubert, E. Weber and N. Dörpinghaus, J. Chem. Soc.,Perkin Trans.2, 2129(1990).
30. E. Weber and H.P. Josel, J. Incl. Phenom., 1,79(1983).
31 M. Otsuka, R. Teraoka and Y. Matsuda, Pharm. Res, 9, 307(1992).

32. H.E. Paul, J.H. Kenyon, M.F. Paul, and A.R. Borgmann, J. Pharm. Sci, 56, 882(1967).
33. E. Shefter and T. Higuchi, J. Pharm Sci., 52, 781(1963).